Published in final edited form as:
Science. 2012 December 7; 338(6112): 1340–1343. doi:10.1126/science.1226135.

Tuning the Electronic Absorption of Protein-Embedded all-*trans*-Retinal

Wenjing Wang, **Zahra Nossoni**, **Tetyana Berbasova**, **Camille T. Watson**, **Ipek Yapici**, **Kin Sing Stephen Lee**, **Chrysoula Vasileiou**, **James H. Geiger***, and **Babak Borhan***
[1]Michigan State University, Department of Chemistry, East Lansing, MI 48824

Abstract

Protein-chromophore interactions are a central component of a wide variety of critical biological processes, such as color vision and photosynthesis. To understand the fundamental elements that contribute to spectral tuning of a chromophore inside the protein cavity, we have redesigned human Cellular Retinol Binding Protein II (hCRBPII) to fully encapsulate all-*trans*-retinal and form a covalent bond as a protonated Schiff base. Using this system, the absorption maximum of the pigment was regulated from 425 nm to 644 nm using rational mutagenesis designed to alter the electrostatic environment within the binding pocket of the host protein. Employing only 9 point mutations, the hCRBPII mutants induce a systematic shift in the absorption profile of all *trans*-retinal of over 200 nm across the visible spectrum.

Light absorbing protein/chromophore complexes play critical roles in a variety of biological processes such as vision, phototaxis and photosynthesis. The function of these systems depends on the modulation of the spectroscopic properties through protein-chromophore interactions. The rhodopsin family represents a particularly interesting case, where the λ_{max} (absorption maximum) of the same chromophore is modulated from 420 nm (human short wave sensitive pigment, hSWS) to 587 nm (sensory rhodopsin I) (1, 2). In all cases, a sole chromophore, retinal in its various isomeric forms, is bound via an iminium (also known as a protonated Schiff base, PSB) through the side chain of a lysine residue (3) to various opsins.

Although the mechanism by which rhodopsins alter the absorbance of a single chromophore (the “opsin shift”) is still debated, it is generally accepted that wavelength regulation is a result of either conformational manipulation of the chromophore, and/or directed electrostatics, where the protein localizes electrostatic potential to various regions of the chromophore [reviewed in (4)]. The latter perturbations lead to stabilization/destabilization of the chromophore’s ground and excited states that greatly influence the absorption profile

*Correspondence to: geiger@chemistry.msu.edu, babak@chemistry.msu.edu.

Additional information and data used in this work can be found in the supplementary materials.

Supplementary Materials
Materials and Methods
Figs. S1–S7, with Supplementary Text
Tables S1–S7, with Supplementary Text
References (21–32)

(5–8). Nonetheless, the iminium in all structurally characterized rhodopsins is stabilized, either directly or through a water-mediated network, by a counteranion, which significantly affects the electrostatic environment of the chromophore (9, 10). In contrast, earlier calculations (11) and gas phase experiments with the retinylidene PSB (12) have indicated that substantial bathochromically shifted spectra would be obtained in a uniformly neutral electrostatic environment in the absence of a PSB counteranion. With the latter principle in mind, we have reengineered proteins capable of binding retinal as a PSB to investigate the details of subtle interactions that can alter the absorption of a bound cationic chromophore. We propose that mutants designed to achieve a more evenly dispersed electrostatic field across the polyene, should lead to ‘super-red’ absorbing pigments in the absence of a counteranion proximal to the iminium nitrogen.

In order to systematically study the correlation between structure and absorption wavelength, we have chosen the Intracellular Lipid Binding Protein family (iLBP), and in particular human Cellular Retinol Binding Protein II (hCRBPII), as the target for protein engineering (13). Tolerance to mutations and the large binding cavity of iLBPs allow flexibility in the redesign of the protein and enable the binding of a wide range of different ligands (14). The relative rigidity of the iLBP fold makes it an ideal scaffold for protein engineering since it is more likely that mutations will not result in structural rearrangement (14), allowing their specific effects to be compared directly. In addition, we have shown that the chromophore must be fully embedded within the binding pocket, since exposure to the aqueous media would buffer electrostatic changes that result from mutations along the polyene (15). As a result of the latter considerations, hCRBPII was specifically chosen from the iLBP family because it fully encapsulates retinal within its binding cavity.

In prior work we showed that the correct trajectory of an active site Lys residue with respect to the electrophilic aldehyde (the Bürgi-Dunitz trajectory) was necessary (16, 17). In that respect, In Silico analysis led to the selection of Gln108 as the suitable position for the active site Lys (Fig. 1A). A second mutation, K40L (Fig. 1A), was required since the positively charged Lys residue inhibited the protonation of the Schiff base formed with retinal. Double mutant Q108K:K40L (KL) binds retinal with high affinity (K_d = 29 ± 5 nM) and yields a PSB with λ_{max} = 508 nm, a 68 nm red-shift as compared to the PSB of retinal in ethanol (λ_{max} = 440 nm). In contrast to the rhodopsins and our earlier engineered protein systems, and confirmed by KL’s crystal structure, a counteranion for the iminium was purposely and successfully omitted. Alternatively, a putative π-cation interaction with Trp106 and the possible interaction with the nearby water network could be stabilizing the protonation of the iminium nitrogen (Fig. 1B).

With KL as the starting point, the electrostatic environment around the chromophore was altered by targeting different zones of the polyene through mutation of nearby amino acids (Fig. 1C). Table 1 illustrates modifications to zones II and III of the bound chromophore. Thr51, Thr53, and Tyr19 were targeted as they were situated relatively close to the polyene (fig. S1). As anticipated, the isosteric replacement of Thr51 in zone III (near the iminium) with a hydrophobic amino acid (Val) led to a substantial red-shift in absorption, presumably by decreasing the negative polarity near the iminium (Table 1 entry 2; fig. S2). Changes to amino acids in zone II (middle of the chromophore) did not produce red-shifted pigments,

highlighted by mutations of Thr53 and Tyr19 with a variety of amino acids, which exhibited maximally a 5 nm red-shift when replaced with Cys and Trp, respectively (Table 1 entries 3 and 5; table S2). A large bathochromic shift was again observed as a result of the T51V mutation when combined with T53C and/or Y19W (Table 1 entries 4, 6 and 7; fig. S3–S4). Changes to zone I (ionone ring end) did not correlate well with electrostatic stabilization of a resonating charge (table S3). In fact, unlike the generally accepted postulate that introduction of negative potential around the ionone ring should lead to more red-shifted pigments [reviewed in (8)], introduction of acidic residues in zones I and II resulted in a blue-shift (tables S2 and S3). In contrast to the rhodopsins and other engineered systems where a counteranion stabilizes the iminium charge, the present system does not require anionic localization at any point along the polyene since there is no strong ionic interaction at the PSB to counterbalance. The absence of a PSB counteranion yields a conjugated system that is more responsive to subtle changes in its environment, enabling greater bathochromic shift by an overall ‘softening’ (more even distribution) of the electrostatic potential along the polyene.

Further gain in uniformly balancing the electrostatic potential along the polyene came from control of the chromophore’s global environment. The dielectric constant inside the binding cavity of proteins is much lower than that of the aqueous environment (estimated to be 2–4 vs. 78) (18). Since exposure to the aqueous environment increases the polarization of the electrostatic potential across the chromophore and also dampens the effect of weakly polarized groups to stabilize a resonating cationic charge, we sought to further sequester the binding pocket. Examination of the hCRBPII structure identified Arg58, located in the entrance of the binding pocket, as a potential ‘leak’ that could be capped with a larger, hydrophobic residue. A number of amino acids were substituted for R58 (table S4a,b); the R58W substitution was the most effective in sequestering the binding pocket from the bulk medium.

Table 1 lists the contribution of the R58W mutation when combined with the KL series of proteins discussed above. A substantial red-shift is observed for these mutants, clearly surpassing the absorption of human long wave sensitive (hLWS) pigment with 6 overall mutations (590 nm, entry 7). Consistent with the idea that solvent exposure can buffer the effect of weakly polarizing amino acids, the R58W containing series of proteins, which have a more sequestered binding pocket, enhance the red-shift of mutations that are introduced far from R58W. For example, T53C and Y19W are ~9 Å from Arg58, yet the R58W mutation yields a much greater red-shift when either T53C or Y19W are present (539 nm → 585 nm for T53C; 537 nm → 577 nm for Y19W). As noted, the same two mutations alone led to smaller bathochromic shifts, suggesting that isolating the interior of the protein from the bulk medium greatly enhances the red-shift induced by substitutions at position 53 and 19. In fact, in all cases, the R58W mutation leads to ~2 fold enhancement in red-shifting of the absorption. Although both Cys and Trp can participate in polar interactions, they are also polarizable and could effectively promote conjugation of the positive charge along the polyene in an environment of low dielectric constant.

Inspection of the crystal structures of all available mutants in the PSB region was invaluable to further optimize the binding pocket (representative structure in Fig. 2A). A water network

that originates from Thr1 to Gln4 and extends to the iminium nitrogen apparently contributes to the stability of the charge on the PSB. Putative disruption of this water network by mutation of Gln4 in KL-T51V:T53C:Y19W:R58W:T29L to Phe, Trp, Leu, Ala, Asn, and Thr all led to bathochromic shift from 591 nm to 610–613 nm (table S5). This was akin to removing a polar amino acid residue, such as Thr51, from zone III. A significant bathochromic shift was gained with the Q4R mutation (622 nm), presumably as a result of increased positive electrostatic potential in zone III, which further destabilizes the localization of the positive charge on the iminium nitrogen. Evident from the crystal structure of KL-T51V:T53C:Y19W:R58W:T29L:Q4R is the absence of the hydrogen bonded water network (Fig. 2B). Although the iminium nitrogen is ~6 Å away from the Arg4 guanidinium, the decreased dielectric constant of the binding pocket translates to higher sensitivity in zone III. Disruption of the putative cation-stabilizing water network was only possible at this late stage of design, having provided the necessary and sufficient means to stabilize the resonating charge along the polyene by earlier mutations. As a point of comparison, the KL:Q4W protein binds retinal to produce a pigment that absorbs maximally at 533 nm, but with a significantly depressed iminium pK_a (8.3 for KL vs. 6.2 for KL:Q4W). This is presumably the result of insufficient stabilizing elements in both the PSB region, and also along the length of the chromophore.

A final push to gain the most bathochromically shifted pigment focused on further encapsulation of the binding pocket from the aqueous environment. The Ala33 position, residing on the α-helix that functions as a lid for ligand entry, provided a likely candidate (Fig. 2C). A series of A33 mutants of the KL-T51V:T53C:Y19W:R58W:T29L:Q4F protein were produced (table S6). Incorporation of A33W led to further red-shifting of the absorption (636 nm), likely as a result of sequestering and increasing the polarizability of the binding pocket (Fig. 2D) (19). The nona-mutant KL-T51V:T53C:Y19W:R58W:T29L:Q4R:A33W produced the most bathochromically shifted retinylidene bound protein complex reported thus far, with a λ_{max} of 644 nm (**M11**, Fig. 3). To put this in context, the most red-shifted retinylidene PSB previously observed (measured in vacuum) peaks at 610 nm, while 620 nm was considered to be the theoretical maximum (12).

Wavelength regulation towards the most red-shifted hCRBPII mutant (644 nm, **M11**) showed that removal of the negative polarity in zone III is necessary. Conversely, introduction of negatively polarized residues in this region should result in a blue-shift by localizing the cation on the iminium nitrogen. Replacement of Lys40 with Ser (**M3**, 482 nm) reverses the polarity in zone III, and produces a blue-shifted pigment relative to KL. Likewise, the absorption of Q108K:T51D double mutant blue-shifted to 474 nm (**M2**). Further, introduction of L117E (also in zone III) generated a significantly hypsochromically shifted mutant (**M1**, 425 nm), which is comparable to hSWS pigment.

The UV-vis spectra and solutions of a number of hCRBPII mutants bound with retinal are shown in Fig. 3. The figure visually depicts the regulation of wavelength of a single chromophore, over a 219 nm range, through the redesign of the electrostatic potential of the protein’s interior. hCRBPII mutants not only recapitulate the wavelength regulation observed with the pigmented rhodopsins, but also red-shift beyond the postulated limit for

any retinylidene PSB. These mutants show that extensive wavelength regulation is possible with little contribution from conformational effects. The latter conclusion was based on the analysis of crystal structures for this series of mutants that show little change in the planarity of the chromophore (fig. S7). As expected, maximal hypsochromicity is achieved by localizing the positive charge on the iminium nitrogen. Extreme bathochromic shifting, on the other hand, depends not on a reversal of polarity but on an even distribution of electrostatic potential across the entire polyene, keeping in mind that a strong interaction of a counteranion to the PSB is not present in these mutants.(20) To this end, it is of utmost importance to not only embed the chromophore within the binding pocket, but to also enclose the binding cavity from the bulk medium, and distribute the cationic charge evenly along the polyene. Embedding the chromophore enables it to respond to electrostatic perturbations and this is enhanced by enclosure of the binding pocket. A balanced distribution of the cationic charge across the polyene is generated by evenly distributed neutral electrostatic potential in the binding pocket, leading to ‘super-red’ pigments.

Supplementary Material

Refer to Web version on PubMed Central for supplementary material.

Acknowledgments

This work was supported by the NIH (Grant No. R01-GM54082). The authors also thank the Department of Energy, Office of Science, Basic Energy Sciences, Chemical Sciences, Geosciences and Biosciences Division (DE-FG02-06ER15822 to J.H.G.). We are grateful to beam line staff at LS-CAT 21-ID (supported by the DOE Office of Energy Research, under Contract No. W-31-109-ENG-38). The APS is supported by the U. S. DOE, Office of Science, Office of Basic Energy Sciences, under Contract No. W-31-109-ENG-38. The PDB accession codes for the crystal structures used in this study are: Q108K:K40L (4EXZ); Q108K:K40L:T51V:T53C:Y19W:R58W:T29L:Q4R (4EEJ); Q108K:K40L:T51V:T53C:Y19W:R58W:T29L:Q4A (4GKC); Q108K:K40L:T51V:T53C:Y19W:R58W:T29L (4EFG); Q108K:K40L:T51V:T53C:Y19W:R58W:T29L:A33W (4EDE).

References and Notes

1. Palczewski K. J. Biol. Chem. 2012; 287:1612. [PubMed: 22074921]
2. Spudich JL, Yang CS, Jung KH, Spudich EN. Annu. Rev. Cell Dev. Biol. 2000; 16:365. [PubMed: 11031241]
3. Palczewski K. Annu. Rev. Biochem. 2006; 75:743–767. [PubMed: 16756510]
4. Nielsen MB. Chem. Soc. Rev. 2009; 38:913. [PubMed: 19421571]
5. Coto PB, Strambi A, Ferre N, Olivucci M. Proc. Natl. Acad. Sci. U. S. A. 2006; 103:17154. [PubMed: 17090682]
6. Kochendoerfer GG, Lin SW, Sakmar TP, Mathies RA. Trends Biochem. Sci. 1999; 24:300. [PubMed: 10431173]
7. Lin SW, et al. J. Biol. Chem. 1998; 273:24583. [PubMed: 9733753]
8. Rajamani R, Lin Y-L, Gao J. J. Comput. Chem. 2011; 32:854. [PubMed: 20941732]
9. Sakmar TP, Franke RR, Khorana HG. Proc. Natl. Acad. Sci., USA. 1989; 86:8309. [PubMed: 2573063]
10. Sakmar TP, Franke RR, Khorana HG. Proc. Natl. Acad. Sci. U. S. A. 1991; 88:3079. [PubMed: 2014228]
11. Honig B, Greenberg AD, Dinur U, Ebrey TG. Biochemistry (Mosc). 1976; 15:4593.
12. Rajput J, et al. Angew. Chem. Int. Ed. 2010; 49:1790.
13. Li E, Norris AW. Annu. Rev. Nutr. 1996; 16:205. [PubMed: 8839926]

14. Gunasekaran K, Hagler AT, Gierasch LM. Proteins-Structure Function and Genetics. 2004; 54:179.
15. Lee KSS, et al. ChemPlusChem. 2012; 77:273.
16. Burgi HB, Dunitz JD. Acc. Chem. Res. 1983; 16:153.
17. Vasileiou C, et al. J. Am. Chem. Soc. 2007; 129:6140. [PubMed: 17447762]
18. Dwyer JJ, et al. Biophys. J. 2000; 79:1610. [PubMed: 10969021]
19. Addition of hydroxylamine to two hCRBPII mutants examined the ability to enclose the binding cavity with mutations of Arg58 and Ala33. Reaction of the retinylidene with hydroxylamine would require ready access of the reagent to the PSB. A rapid disappearence of the PSB was observed upon addition of hydroxylamine to the hCRBPII mutant that retained Arg58 and Ala33. Conversely, the protein contaning the R58W and A33W mutations resisted change in the presence of hydroxylamine (see SOM for further details)
20. The calculated electrostatic potential of **M10** (622 nm) projected onto the bound retinylidine chromophore is compared to that of **M4** (508 nm) in Figure S5. The comparison illustrates that to achieve the red-shift observed in **M10**, the chromophore experiences an even distribution of a neutral electrostatic potential across its length.

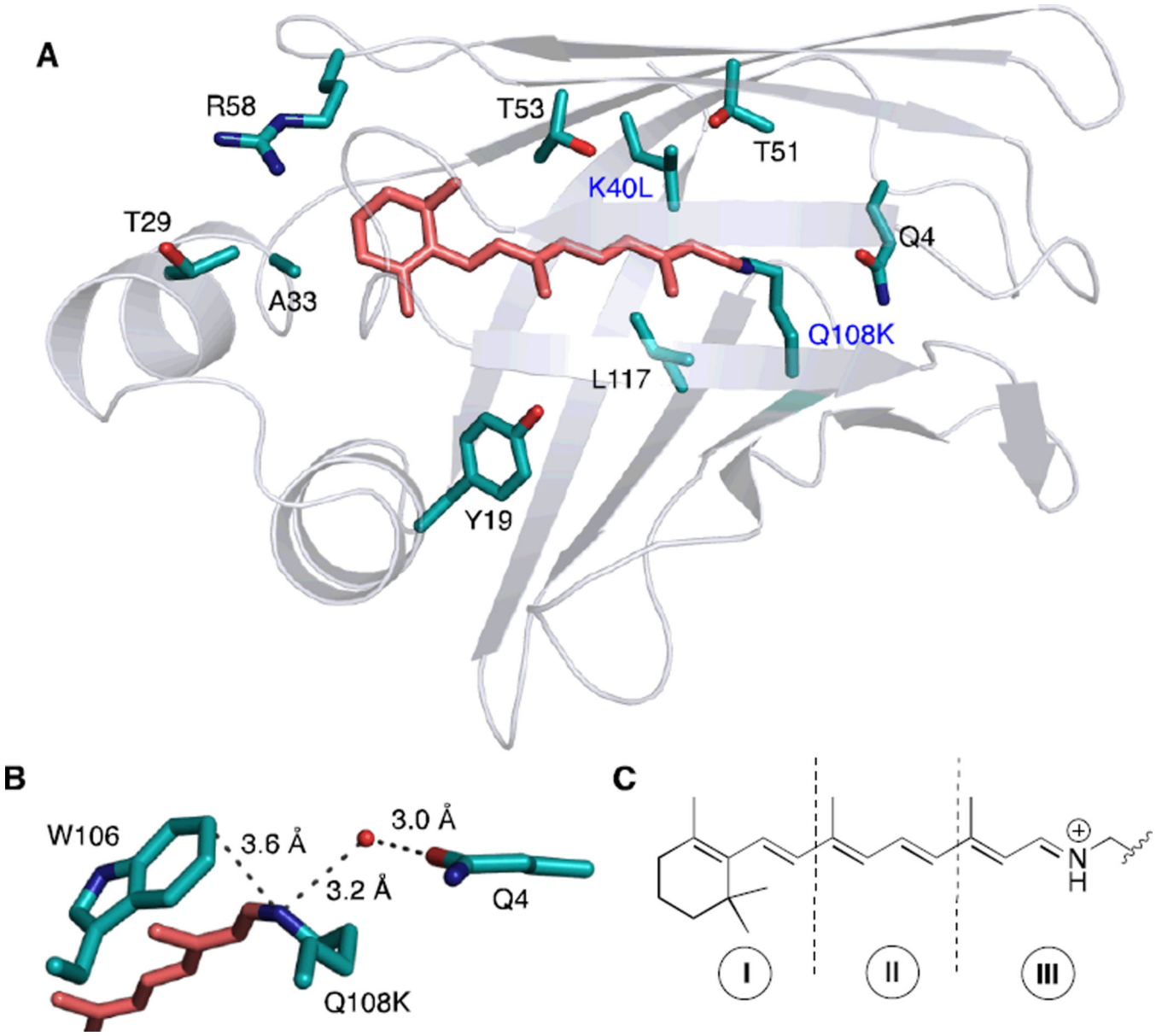

Figure 1.

A. Crystal structure of Q108K:K40L-hCRBPII, with residues most pertinent to this study highlighted. **B.** Trp106 and a close lying water molecule hydrogen bonded to Gln4 putatively stabilize the protonation of the iminium without the presence of a counteranion. **C.** Protonated Schiff base (PSB) of all-*trans*-retinal. The chromophore is divided into three segments to clarify the discussion of mutations that are close to different locations of the polyene.

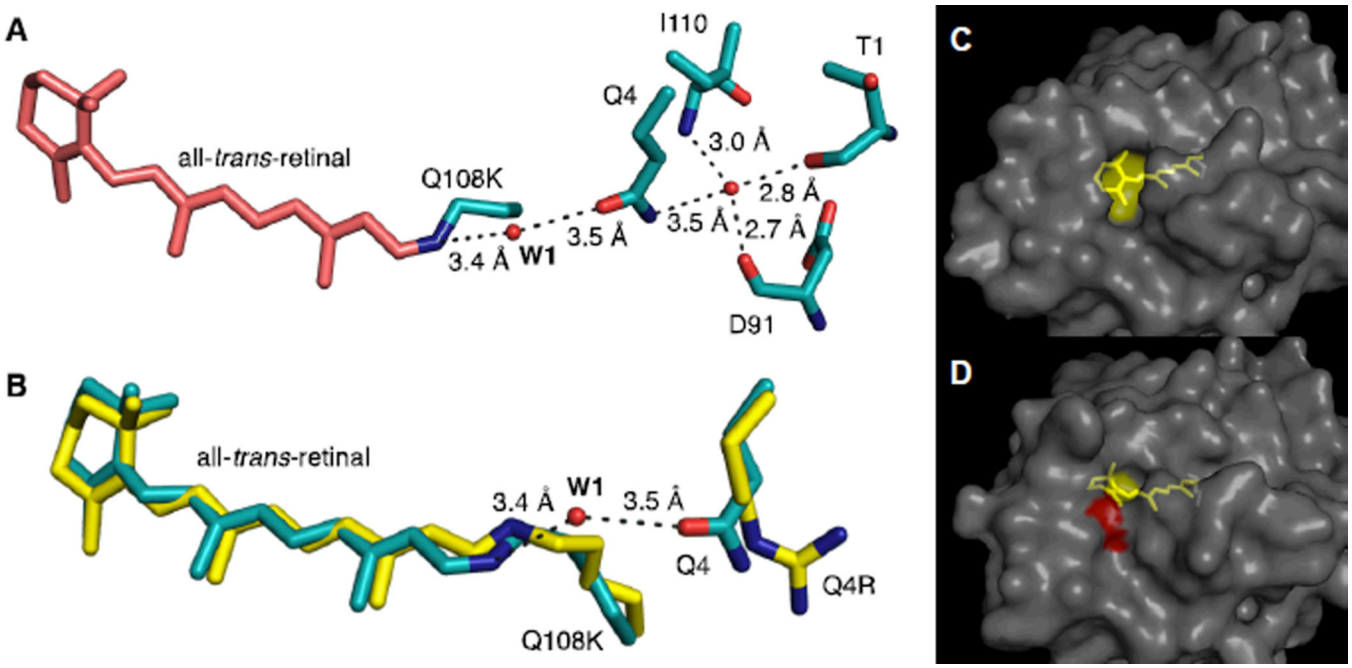

Figure 2.

A. Crystal structure of Q108K:K40L:T51V:T53C:Y19W: R58W:T29L hCRBPII with Thr1, Gln4, Asp91, and Ile110 highlighted to show hydrogen bonding to W1, extending to the iminium nitrogen. **B**. The overlay of the crystal structures of Q108K:K40L:T51V:T53C:Y19W:R58W :T29L hCRBPII (591 nm, cyan structure) and Q108K:K40L: T51V:T53C:Y19W:R58W:T29L:Q4R hCRBPII (622 nm, yellow structure) indicating the lack of an ordered water molecule with the Q4R mutant that leads to further bathochromic shift of the retinylidene protein complex. As exemplified in the latter two structures, all mutants that have an ordered water molecule adopt the *cis*-imine geometry. Conversely, *trans*-imine geometry is observed in all Q4 mutants without the ordered water molecule (fig. S7). **C**. Crystal structure of Q108K:K40L:T51V:T53C:Y19W: R58W:T29L hCRBPII (591 nm) illustrates the opening near Ala33. **D**. Crystal structure of Q108K:K40L:T51V:T53C:Y19W:R58W:T29L:**A33W** hCRBPII (606 nm) shows substantial closing of the orifice (A33W surface shown in red).

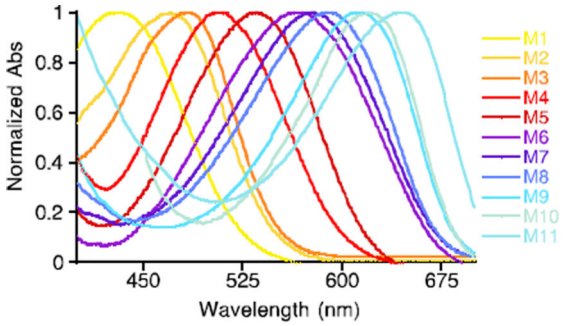

Entry	Pigments	λ_{max} nm	Protein shift nm (cm^{-1})[a]	K_d, nM[b]
1	*n*Bu-retinylidene PSB	440	---	---
2	hSWS	420	-20 (-1,082)	---
M1	Q108K:T51D:L117E	425	-15 (-802)	53±15
M2	Q108K:T51D	474	34 (1,630)	23±6
M3	Q108K:K40S	482	42 (1,980)	28±12
3	sensory rhodopsin II	487	47 (2,193)	---
4	rod-rhodopsin	500	60 (2,727)	---
M4	Q108K:K40L	508	68 (3,042)	29±5
5	hMWS	530	90 (3,859)	---
M5	Q108K:K40L:T51V	533	93 (3,966)	19±7
6	hLWS	560	120 (4,870)	---
7	bacteriorhodopsin	570	130 (5,183)	---
M6	Q108K:K40L:T51V:R58W	570	130 (5,183)	63±4
M7	Q108K:K40L:T51V:Y19W:R58W	577	137 (5,396)	86±6
8	sensory rhodopsin I	587	147 (5,691)	---
M8	Q108K:K40L:T51V:T53C:Y19W:R58W:T29L	591	150 (5,778)	55±5
M9	Q108K:K40L:T51V:T53C:Y19W:R58W:T29L:Q4W	613	173 (6,414)	65±8
M10	Q108K:K40L:T51V:T53C:Y19W:R58W:T29L:Q4R	622	182 (6,650)	70±6
M11	Q108K:K40L:T51V:T53C:Y19W:R58W:T29L:Q4R:A33W	644	204 (7,199)	42±6

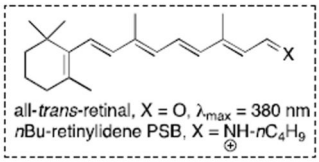

[a]Protein shift is defined as the difference between the absorbance of *n*-butylamine retinylidene protonated Schiff base and the absorbance of retinal-bound hCRBPII mutants; wavenumbers given in parantheses provide a direct correlation to the change in energy. [b]The binding constants for the hCRBPII mutants (presented as dissociation constants K_d), indicate strong binding of retinal with the proteins.

Figure 3.

Normalized UV-vis spectra of a selected group of hCRBPII mutants (**M1**-**M11**) are displayed. As indicated in the table, the absorption of the mutants spans from 425 nm (**M1**) to 644 nm (**M11**). For comparison, the wavelengths of various rhodopsins are included. The pigments in the cuvettes were generated by incubation of all-*trans*-retinal (72 μM in 100 mM phosphate buffer, pH 7.3, shown in the left cuvette) with hCRBPII mutants **M1**-**M11** (80 μM protein, same concentration of retinal was used in all cuvettes).

Table 1

Q108K:K40L hCRBPII (KL)-based mutants.

Entry	Zone	hCRBPII mutant	λ_{max}, nm R58	Protein shift nm (cm^{-1})[a]	λ_{max}, nm R58W	Protein shift nm (cm^{-1})[b]	Enhancement nm[c]
1	---	KL	508	0 (0)	527	0 (0)	---
2	III	KL:**T51V**	533	25 (923)	570	43 (1,431)	18 (1.7x)
3	II	KL:**T53C**	513	5 (192)	540	13 (457)	8 (2.6x)
4	II+III	KL:**T51V:T53C**	539	31 (1,132)	585	58 (1,881)	27 (1.9x)
5	II	KL:**Y19W**	513	5 (192)	538	11 (388)	6 (2.2x)
6	II+III	KL:**T51V:Y19W**	537	29 (1,063)	577	50 (1,644)	21 (1.7x)
7	II+III	KL:**T51V:T53C:Y19W**	538	30 (1,098)	590	63 (2,026)	33 (2.1x)

[a] protein shift with reference to Q108K:K40L, wavenumbers given in parantheses provide a direct correlation to the change in energy;

[b] protein shift with reference to Q108K:K40L:R58W;

[c] Enhancement is calculated as the difference in protein shift between KL-R58W mutants and the KL mutants, and reflects the overall increased red-shift in excess of that anticipated from a purely additive effect of R58W. For example, the T51V mutation leads to a 25 nm bathochromic shift (KL vs KL:T51V). A 25 nm red-shift would be expected for KL:T51V:R58W vs KL:R58W, however, a 43 nm shift is observed. The 18 nm difference in the level of enhancement (1.7 fold increase) as a result of the R58W mutation. The number in the parenthesis for column labeled ‘enhancement’ is the fold increase of the protein shift of the KL-R58W mutant series with respect to the KL mutant series.